Multiple Target Tracking Using Particle Filtering and Adaptive Waveform Design

I. Kyriakides*, T. Trueblood**, Darryl Morrell***, and A. Papandreou-Suppappola**
*Department of Engineering, University of Nicosia, Nicosia, Cyprus
**Department of Engineering, Arizona State University, Mesa, AZ 85212, USA
**Department of Electrical Engineering, Arizona State University, Tempe, AZ 85287, USA
E-mail: kyriakides.i@unic.ac.cy, ttrueblo@asu.edu, morrell@asu.edu, papandreou@asu.edu

***Abstract*—In multiple target tracking with radar, weak target measurements are often hard to observe due to masking by sidelobes of measurements from stronger targets. The result is lost tracks and deteriorated joint tracking performance. In this work, we design configurable waveforms and adjust the positioning of their ambiguity function (AF) sidelobes to unmask weak targets and improve tracking performance. To track multiple targets, we develop a tracker that is based on the likelihood particle filter and the independent partitions proposal method. The proposed independent partitions likelihood particle filter (IPLPF) accurately processes the high resolution measurements resulting from the use of Björck CAZAC sequences that we use to construct our configurable waveforms and tracks a fixed and known number of targets. We provide simulation results that demonstrate the improvement in tracking performance of multiple targets when using adaptively configured MCPC Björck CAZAC waveforms versus using non-adaptive configurations or single Björck CAZACs.**

I. Introduction

When tracking multiple targets with radar sensors, weak targets are often difficult to observe. This is because the sidelobes of the AFs of strong targets are higher than the main sidelobe AFs of the weak targets in the delay-Doppler plane. As a result, the joint tracking performance of a multitarget tracker, expressed either in terms of mean squared error or percentage of lost tracks, is low. In this paper, we design configurable radar waveforms and develop an adaptive radar sensor configuration technique to position strong target sidelobes away from predicted locations of weak targets.

In the literature, the delay-Doppler plane is overlaid with rectangularly shaped resolution cells placed on a fixed grid in order to process the return signal. In [1], these cells are constructed in such way as to approximate the shape of the probability of detection contour that depends on the signal type and its parameters. Instead of using a fixed waveform, adaptive waveform techniques were used to minimize either the tracking error or the validation gate volume in [2]. However, these techniques rely on linear observation models that do not accurately represent physical systems with non-linear characteristics.

In this work, we develop a tracker that collects measurements according to the predicted target state instead of a fixed grid for linear systems to track a known and fixed number of targets. The tracker is based on the independent partitions algorithm [3] and the likelihood particle filter [4]. We also construct multicarrier phase-coded (MCPC) waveforms [5] based on Björck constant amplitude zero-autocorrelation (CAZAC) [6] sequences with sidelobes positioned to reveal weak targets and, thus, improve tracking performance.

The rest of the paper is organized as follows. In Section II, we develop the MCPC Björck CAZACs, and we investigate the properties of their AFs. In Section III, we we describe the IPLPF algorithm and in Section IV we discuss the waveform configuration algorithm. We also conduct a simulations of tracking ground targets with radar sensors in Section V.

II. MCPC CAZAC Sequences

Our objective is to design waveforms whose AF can be adaptively selected in such way as to unmask weak targets in multitarget tracking scenarios. Moreover, we design AF surfaces with large regions of zero sidelobes in order to be able to unmask weak target measurements in the presence of strong target measurement sidleobes. We combine different cyclically shifted CAZACs in frequency with AF surfaces that have sidelobes whose locations depend on the difference in cyclic shift, the number of sequences, and their length. A cyclically permuted Björck CAZAC sequence is given by $s(m)w^{\frac{m\kappa}{M}}$ where $w = e^{j2\pi}$ and κ is the frequency shift. We combine Q cyclically permuted Björck CAZACs,

$$s_q(m) = s(m)w^{\frac{m\kappa_q}{M}} \tag{1}$$

where $q = 0, \ldots, Q-1$ using the multicarrier phase coded scheme. MCPC waveforms [5] are constructed using orthogonal frequency division multiplexing (OFDM). The AF [1] of a Björck CAZAC waveform $s(m), m = 0, \ldots, M-1$, is defined as:

$$\mathcal{A}_s(\tau,\nu) = \frac{1}{E_s}\frac{1}{M}\sum_{m=0}^{M-1} s(m-\tau)w^{\frac{m\nu}{M}}s^*(m) \tag{2}$$

where τ and ν represent the discrete delay and Doppler and $E_s = \frac{1}{M}\sum_{m=0}^{M-1} s(m)s^*(m)$ is the energy of $s(m)$.

The MCPC CAZAC waveform, modulated with carrier frequency κ_c, is given by [1]

$$g_{\mathbf{\Theta}}(m) = \frac{1}{\sqrt{Q}}\sum_{q=0}^{Q-1} s_q(\lfloor\frac{m}{Q}\rfloor)w^{-\frac{qm}{Q}}w^{\frac{m\kappa_c}{QM}} \tag{3}$$

This work was supported under MURI Grant No. AFOSR FA9550-05-1-0443.

[1]The notation $\lfloor . \rfloor$ denotes rounding down to the nearest integer

where $m = 0, \ldots, MQ-1$. Note that the sampling rate of the MCPC CAZAC is increased by Q as compared with the sampling rate of the SCPC CAZAC. The vector $\mathbf{\Theta} = (Q, M, \kappa)$ defines the parameters of the MCPC waveform. We choose to restrict $\kappa_q = \kappa q$ where $\kappa = 0, \ldots, M-1$. This selection of cyclic frequency shifts causes the positioning of the sidelobes of the AF to depend on κ. The AF surface of the MCPC Björck CAZAC is computed as

$$|\mathcal{A}_{g_{\mathbf{\Theta}}}(\tau,\nu)|^2 = |\frac{1}{E_{g_{\mathbf{\Theta}}}}\frac{1}{MQ}\sum_{m=0}^{MQ-1} g_{\mathbf{\Theta}}(m-\tau)w^{-\frac{m\nu}{QM}}g^*_{\mathbf{\Theta}}(m)|^2$$

where $E_{g_{\mathbf{\Theta}}} = \frac{1}{MQ}\sum_{m=0}^{MQ-1} g_{\mathbf{\Theta}}(m)g^*_{\mathbf{\Theta}}(m)$ is the energy of $g_{\mathbf{\Theta}}(m)$ which is normalized to have the same energy as $s(m)$. Using (1) and (3) the AF surface becomes

$$|\mathcal{A}_{g_{\mathbf{\Theta}}}(\tau,\nu)|^2 = |\frac{1}{E_{g_{\mathbf{\Theta}}}}\frac{1}{MQ^2}\sum_{m=0}^{MQ-1} s(\lfloor\frac{m-\tau}{Q}\rfloor)w^{-\frac{m\nu}{QM}}s^*(\lfloor\frac{m}{Q}\rfloor)$$
$$\cdot\sum_{q=0}^{Q-1} w^{\frac{\lfloor\frac{m-\tau}{Q}\rfloor(\kappa q)M}{M}}w^{-\frac{q(m-\tau)}{Q}}\sum_{\hat{q}=0}^{Q-1} w^{-\frac{\lfloor\frac{m}{Q}\rfloor(\kappa\hat{q})M}{M}}w^{\frac{\hat{q}m}{Q}}|^2 \quad (4)$$

We consider two special cases that provide AF surfaces with sidelobes that can be conveniently positioned by adjusting the waveform parameters. As shown in [7], for the case when $\kappa = 0$ we have zero AF surface regions of width Q (see Figure 1) and for the case when $\kappa = 1$ we have zero AF surface regions of width $Q + \frac{Q}{M}$.

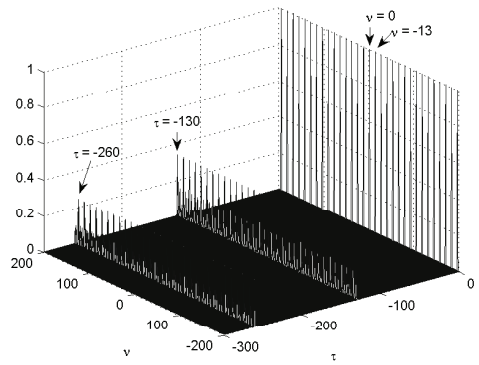

Fig. 1. AF surface plot of an MCPC Björck CAZAC with parameters $\mathbf{\Theta} = (Q, M, \kappa) = (130, 13, 0)$.

In summary, the possibility to choose the parameters $\mathbf{\Theta} = (Q, M, \kappa)$ of an MCPC Björck CAZAC waveform and also to rotate the entire AF surface by choosing to take the FT of the waveform enables us to position sidelobes in order to minimize the predicted mean squared error as shown in Section IV.

III. Independent Partition Likelihood Particle Filter Algorithm

A. Tracking Scenario

1) Motion Model: We consider a fixed and known number of targets, denoted by L, moving in a two-dimensional plane. The dynamics of each target are modeled by a nearly constant velocity motion model [8] in Cartesian coordinates. Specifically, the state vector for the lth target, $l = 1, \ldots, L$, at time step k, $k = 1, ..., K$, is given by $\mathbf{x}_{l,k} = [x_{l,k}\ \dot{x}_{l,k}\ y_{l,k}\ \dot{y}_{l,k}]^T$ where $x_{l,k}$, $y_{l,k}$ are the positions in the x and y directions, and $\dot{x}_{l,k}$, $\dot{y}_{l,k}$ are the corresponding velocities. The motion is formulated as:

$$\mathbf{x}_{l,k} = \mathbf{F}\mathbf{x}_{l,k-1} + \mathbf{v}_{l,k} \quad (5)$$

where $\mathbf{F} = [1, \Delta t, 0, 0; 0, 1, 0, 0; 0, 0, 1, \Delta t; 0, 0, 0, 1]$ and Δt is the time difference between observations. $\mathbf{v}_{l,k}$ is a white, zero mean vector Gaussian process with covariance matrix $\mathbf{Q}$ that models target deviations from constant velocity; in this work, we restrict $\mathbf{Q}$ to be diagonal. Therefore, we define $\mathbf{Q} = \text{diag}([\sigma_x^2, \sigma_y^2, \sigma_{\dot{x}}^2, \sigma_{\dot{y}}^2])$. The model in (5) can be used to determine the kinematic prior distribution $p(\mathbf{x}_{l,k}|\mathbf{x}_{l,k-1})$ for target l.

The multitarget state vector is expressed in terms of the state vectors of each target as $\mathbf{X}_k = [\mathbf{x}_{1,k}^T\ \mathbf{x}_{2,k}^T\ \ldots\ \mathbf{x}_{L,k}^T]^T$ where $\mathbf{x}^T$ denotes the transpose of $\mathbf{x}$. Following [3], we refer to each component $\mathbf{x}_{l,k}$ of the state vector $\mathbf{X}_k$ as a partition. Since we assume that the targets move independently, the multitarget kinematic prior distribution is given by $p(\mathbf{X}_k|\mathbf{X}_{k-1}) = \prod_{l=1}^{L} p(\mathbf{x}_{l,k}|\mathbf{x}_{l,k-1})$.

2) Measurement Model: We use U sensors that operate independently, transmitting and receiving waveforms. Specifically, assuming point targets, for partition l at time step k, the range and range rate relative to sensor $u = 1, \ldots, U$ are given respectively by [9] $r_{l,u,k} = \sqrt{(\chi_u - x_{l,k})^2 + (\psi_u - y_{l,k})^2}$, $\dot{r}_{l,u,k} = (\dot{x}_{l,k}(x_{l,k} - \chi_u) + \dot{y}_{l,k}(y_{l,k} - \psi_u))/r_{l,k}$, where χ_u and ψ_u are the Cartesian coordinates of sensor u. It follows that the return signal will contain delayed and Doppler shifted replicas of the transmitted signal due to each target, with discrete delays and Doppler shifts given respectively by the expressions [9] $\tau_{l,u,k} = \text{round}(\frac{2r_{l,u,k}}{cT_b})$, $\nu_{l,u,k} = \text{round}(\frac{-2f_c\dot{r}_{l,u,k}}{cMT_b})$ where round$(\cdot)$ signifies rounding to the nearest integer, c is the velocity of propagation, f_c is the carrier frequency, and T_b is the sampling period.

3) Return Signal and Matched Filter Statistic: We assume that at every time step k, a signal $s(m), m = 0, \ldots, M-1$, where M is the total number of samples of the waveform, is simultaneously transmitted from each of the U sensors in different frequency bands to avoid interference. The sum of the return signals to each sensor u that are reflected from each of the L targets at the discrete delay and Doppler locations $\tau_{l,u,k}$ and $\nu_{l,u,k}$, respectively, is $d_{u,k}(m) = \sum_{l=1}^{L} A_{l,u,k}s(m - \tau_{l,u,k})w^{\frac{m\nu_{l,u,k}}{M}}w^{\frac{(m-\tau_{l,u,k})\kappa_c}{M}} + v_{u,k}(m)$ where κ_c is the discrete carrier frequency with which $s(m)$ is transmitted. The factor $A_{l,u,k}$ is a sum of random complex returns from many different target scatterers on target l, according to the Swerling I model [10]. Therefore, $A_{l,u,k}$ is assumed to be zero-mean, complex Gaussian with known variance $2\sigma_{A,l}^2$. In this work, it is assumed that we are tracking targets with different radar cross sections [11], therefore, targets with different strengths in their return signal. Here, the strength of the target is represented by the variance of $A_{l,u,k}$. The noise terms $v_{u,k}(m)$ for $u = 1, \ldots, U$ are assumed to be zero-mean

complex Gaussian with variance $2N_0$ and independent for each sensor u. Here, we also define the signal-to-noise ratio (SNR) to be SNR $= \frac{\sigma^2_{A,l_w} E_s}{N_0}$ [1] where l_w is the index of the weakest target and E_s the energy of the transmitted waveform. The demodulated discrete representation of the waveform at the receiver is given by $d_{u,k}(m) = \sum_{l=1}^{L} A_{l,u,k} s(m - \tau_{l,u,k}) w^{\frac{m\nu_{l,u,k}}{M}} w^{-\frac{\tau_{l,u,k}\kappa_c}{M}} + v_{u,k}(m)$. The return signal is filtered to match a template signal representing returns from Λ targets, at different delay and Doppler locations $\tilde{\tau}_{\lambda,u,k}$, $\tilde{\nu}_{\lambda,u,k}$, $\lambda = 1, \ldots, \Lambda$, respectively. These delay and Doppler locations are derived from the belief in target state as represented by the particles of a particle filtering approach. We will let Λ to equal L or 1, depending whether we are proposing particles with L partitions or independently proposing a single partition. Given a set of delay and Doppler values $\{\tilde{\tau}_{\lambda,u,k}\}$ and $\{\tilde{\nu}_{\lambda,u,k}\}$, the matched filter output $\tilde{\mathbf{y}}_{u,k}$ is formed as $\tilde{\mathbf{y}}_{u,k} = \sum_{l=1}^{L} \sum_{\lambda=1}^{\Lambda} A_{l,k} E_s \mathcal{A}_s(\tilde{\tau}_{\lambda,u,k} - \tau_{l,u,k}, \nu_{l,u,k} - \tilde{\nu}_{\lambda,u,k}) w^{-\frac{\tau_{l,u,k}\kappa_c}{M}} + \frac{1}{M} \sum_{m=0}^{M_d} v_{u,k}(m) \sum_{\lambda=1}^{\Lambda} s^*(m - \tilde{\tau}_{\lambda,u,k}) w^{-\frac{m\tilde{\nu}_{\lambda,u,k}}{M}}$ where we have used (2). $M_d > M$ should be large enough to accommodate a maximum delay of a signal reflected from a target. The matched filter statistic that we will use for estimation is given by $\mathbf{y}_{u,k} = |\tilde{\mathbf{y}}_{u,k}|^2$. Since $\tilde{\mathbf{y}}_{\tilde{\tau},\tilde{\nu},u,k}$ is complex Gaussian, the matched filter statistic $\mathbf{y}_{u,k} = |\tilde{\mathbf{y}}_{u,k}|^2$ is exponentially distributed and the measurement likelihood is given by

$$p_\mu(\mathbf{y}_{u,k}|\mathbf{x}_k) = \frac{1}{2\sigma_\mu^2} e^{-\frac{\mathbf{y}_{u,k}}{2\sigma_\mu^2}} \tag{6}$$

where $\mu = 0, 1$ signify target presence or absence respectively. The single partition likelihoods are

$$p_\mu(\mathbf{y}_{\lambda,u,k}|\mathbf{x}_k) = \frac{1}{2\sigma_{\lambda,\mu}^2} e^{-\frac{\mathbf{y}_{\lambda,u,k}}{2\sigma_{\lambda,\mu}^2}} \tag{7}$$

B. Likelihood Partition Sampling and Particle Weighting

Next, we show the process of sampling from the likelihood needed to process the high resolution measurements from the use of Björck CAZAC sequences. The IPLPF functions as follows. We evaluate likelihood values at discrete bins of the delay-Doppler space for each partition independently. We then create a histogram from these values and sample partition states from it. We narrow, however, our selection of bins to a region in which a partition sample from the kinematic prior would fall with probability of almost 1. This way, the number of bins required to build the histogram is reduced and the sample from the measurements is made consistent with the kinematic prior. We then evaluate partition weights by combining measurements from the different sensors and using the kinematic prior. Using the normalized partition weights we sample values for each partition independently. Next, we combine the sampled partitions into particles. The proposal of partitions is followed by the weighting of particles, estimation and particle resampling.

We begin by propagating the $\chi - \psi$ coordinate components of each partition λ of the state space without the addition of noise. We denote with λ the partition that we currently propose and with l the partition that represents the true state of the lth target:

$$\check{\mathbf{x}}^n_{\lambda,k} = [\check{x}^n_{\lambda,k}, \check{y}^n_{\lambda,k}, \check{\dot{x}}^n_{\lambda,k}, \check{\dot{y}}^n_{\lambda,k}]^T = \mathbf{F}\mathbf{x}^n_{\lambda,k-1}. \tag{8}$$

Using $\check{\mathbf{x}}^n_{\lambda,k}$ we have:

$$\check{r}^n_{\lambda,u,k} = \sqrt{(\chi_u - \check{x}^n_{\lambda,k})^2 + (\psi_u - \check{y}^n_{\lambda,k})^2}. \tag{9}$$

Next we determine a region of delay-Doppler bins that could contain observations if the true state is $\check{\mathbf{x}}^n_{\lambda,k}$. If we assume that $(\sigma_x^2 = \sigma_y^2)$, the proposed particle will likely to fall in the regions [7]:

$$[\tau^n_{min,\lambda,u,k}, \tau^n_{max,\lambda,u,k}] = [\lfloor \frac{2r^n_{min,\lambda,u,k}}{cT} \rfloor, \lceil \frac{2r^n_{max,\lambda,u,k}}{cT} \rceil] \tag{10}$$

With a similar procedure for the Doppler we have:

$$[\nu^n_{min,\lambda,u,k}, \nu^n_{max,\lambda,u,k}] = [\lfloor \frac{-2f_c\dot{r}^n_{min,\lambda,u}}{c\Delta\nu} \rfloor, \lceil \frac{-2f_c\dot{r}^n_{max,\lambda,u}}{c\Delta\nu} \rceil]. \tag{11}$$

We form the set

$$\{\{\tau^n_{i_\tau,\lambda,u,k}, \nu^n_{i_\nu,\lambda,u,k}\}\}, \tag{12}$$

where $i_\tau = 0, \ldots, I^n_\tau$ $i_\nu = 0, \ldots, I^n_\nu$ and $I^n_\tau = \tau^n_{max,\lambda,u,k} - \tau^n_{min,\lambda,u,k}$, $I^n_\nu = \nu^n_{max,\lambda,u,k} - \nu^n_{min,\lambda,u,k}$ containing all combinations of indices for delay and Doppler that lie within the delay and Doppler minimum and maximum values, where each index pair is given by:

$$\{\tau^n_{i_\tau,\lambda,u,k}, \nu^n_{i_\nu,\lambda,u,k}\} = \{\tau^n_{min,\lambda,u,k} + i_\tau, \nu^n_{min,\lambda,u,k} + i_\nu\}$$

$$i_\tau = 0, \ldots, I^n_\tau, i_\nu = 0, \ldots, I^n_\nu \tag{13}$$

Evaluating the matched filter output (where the subscript k is omitted for simplicity) at each of these values, and for sensors $u = 1, 2$, we have:

$$\mathbf{y}^n_{i_\tau,i_\nu,\lambda,u} = |\sum_{l=1}^{L} A_l E_s \mathcal{A}(\tau^n_{i_\tau,\lambda,u} - \tau_{l,u}, \nu_{l,u} - \nu^n_{i_\nu,\lambda,u})$$

$$\cdot w^{-\frac{\tau_{\lambda,u}\kappa_c}{M}} + \frac{1}{M} \sum_{m=0}^{M_d} v_u(m) s^*(m - \tau^n_{i_\tau,\lambda,u}) w^{-\frac{m\nu^n_{i_\nu,\lambda,u}}{M}}|^2. \tag{14}$$

Above we have used only one delay-Doppler pair $(\tau^n_{i_\tau,\lambda,u,k}, \nu^n_{i_\nu,\lambda,u,k})$ in the template signal representing a single partition (λ). The single partition likelihood for each delay-Doppler bin $\{\tau^n_{i_\tau,\lambda,u,k}, \nu^n_{i_\nu,\lambda,u,k}\}$ is then given by:

$$p^n_\mu(\mathbf{y}^n_{i_\tau,i_\nu,\lambda,u}|\tau^n_{i_\tau,\lambda,u,k}, \nu^n_{i_\nu,\lambda,u,k}) = \frac{1}{2\sigma^2_{\lambda,\mu}} e^{-\frac{\mathbf{y}^n_{i_\tau,i_\nu,\lambda,u,k}}{2\sigma^2_{\lambda,\mu}}} \tag{15}$$

where $\mu = 0, 1$ signify target presence or absence respectively. We evaluate the likelihood ratio for each delay-Doppler bin $\{\tau^n_{i_\tau,\lambda,u,k}, \nu^n_{i_\nu,\lambda,u,k}\}$ as

$$\check{\beta}^n_{i_\tau,i_\nu,\lambda,u} = \frac{p^n_1(\mathbf{y}^n_{i_\tau,i_\nu,\lambda,u}|\tau^n_{i_\tau,\lambda,u,k}, \nu^n_{i_\nu,\lambda,u,k})}{p^n_0(\mathbf{y}^n_{i_\tau,i_\nu,\lambda,u}|\tau^n_{i_\tau,\lambda,u,k}, \nu^n_{i_\nu,\lambda,u,k})}. \tag{16}$$

The normalized distribution and the normalization factor are respectively

$$\check{B}^n_{\lambda,u} = \sum_{i_\tau=0}^{I^n_\tau} \sum_{i_\nu=0}^{I^n_\nu} \check{\beta}^n_{i_\tau,i_\nu,\lambda,u} \tag{17}$$

$$\check{b}^n_{i_\tau,i_\nu,\lambda,u} = \frac{\check{\beta}^n_{i_\tau,i_\nu,\lambda,u}}{\check{B}^n_{\lambda,u}}. \tag{18}$$

We then sample indices $j^n_{i_\tau,u}, j^n_{i_\nu,u} \sim \{\{\check{b}^n_{i_\tau,i_\nu,\lambda,u}\}^{I^n_\tau}_{i_\tau=0}\}^{I^n_\nu}_{i_\nu=0}$, for each particle n and each sensor $u = 1, 2$. The resulting sampled range and range rate and the bias are respectively: $r^n_{i'_\tau,i'_\nu,\lambda,u} = \frac{c\tau^n_{j_{i_\tau},\lambda,u,k}T_b}{2}$, $\dot{r}^n_{i'_\tau,i'_\nu,\lambda,u} = -\frac{c\nu^n_{j_{i_\nu},\lambda,u,k}\Delta\nu}{2f_c}$, $b^n_{i'_\tau,i'_\nu,\lambda,u} = \check{b}^n_{j_{i_\tau},j_{i_\nu},\lambda,u}$. The values of $r^n_{i'_\tau,i'_\nu,\lambda,u}$ and $\dot{r}^n_{i'_\tau,i'_\nu,\lambda,u}$, in turn, yield proposed state values for location and velocity in the $\chi-\psi$ coordinates $\tilde{\mathbf{x}}^n_{\lambda,k}$. This is accomplished by taking the intersection of two circles in the Cartesian plane and choosing the intersection point in Euclidian distance to the propagated $\chi-\psi$ coordinate locations for partition λ, $\check{x}^n_{\lambda,k}, \check{y}^n_{\lambda,k}$ (i.e. the location that mostly agrees with the kinematic prior information). We note that the so far sampled partitions $\tilde{\mathbf{x}}^n_{\lambda,k}$ are based on information provided from only two sensors. Therefore, some of these partitions may be erroneous, as we explained in the introduction of this section. However, the values $\tilde{\mathbf{x}}^n_{\lambda,k}$ now allow us to easily evaluate the likelihoods for each of the three sensors in order to sample partitions in the next stage of the proposal where we use the information provided by the third sensor and the IP [3] method of sampling partitions to remove partitions that have been erroneously sampled as described in [7] in more detail.

After partition resampling with the IP method, we assemble particles from the sampled partitions as $\mathbf{X}^n_k = [{\mathbf{x}^n_{1,k}}^T \dots {\mathbf{x}^n_{L,k}}^T]^T$. In particle weighting, we weight these particles with weights that incorporate prior and measurement information. The expression for the weight equation for particle n' is given by [7] as

$$\Gamma^{n'}_k = \frac{\Gamma^{n'}_{k-1}}{W_k} \frac{\prod^U_{u=1} p_1^{n'}(\mathbf{y}^{n'}_{u,k}|\mathbf{X}^{n'}_k) p(\mathbf{X}^{n'}_k|\mathbf{X}^{n'}_{k-1})}{\prod^U_{u=1} p_0^{n'}(\mathbf{y}^{n'}_{u,k}|\mathbf{X}^{n'}_k) \prod^\Lambda_{\lambda=1} b^{n'}_{\lambda,k}} \tag{19}$$

where

$$\mathbf{y}^n_u = |\sum^L_{l=1}\sum^\Lambda_{\lambda=1} A_l E_s \mathcal{A}(\tau^n_{\lambda,u} - \tau_{l,u}, \nu_{l,u} - \nu^n_{\lambda,u}) w^{-\frac{\tau_{l,u}\kappa_c}{M}} + \frac{1}{M}\sum^{M_d}_{m=0} v_u(m) \sum^\Lambda_{\lambda=1} s^*(m - \tau^n_{\lambda,u}) w^{-\frac{m\nu^n_{\lambda,u}}{M}}|^2. \tag{20}$$

For the above expression of the weight equation we used the assumption that measurements originating from different particle proposed positions are independent [7], [12].

IV. Adaptive Waveform Selection

In order to improve tracking performance, we select at each time step k the set of parameters $\mathbf{\Theta}_k = (Q, M, \kappa)$ of the transmitted MCPC CAZAC waveform to minimize the predicted mean squared tracking error. The tracking error cost function depends on the unknown state $\mathbf{X}_k$ and the set of measurements that will result from the use of the waveform with a set of parameters $\mathbf{\Theta}_k$. Moreover, the cost function will depend on the estimate of the multitarget state $\hat{\mathbf{X}}_k = \sum^N_{n=1} \Gamma^n_k \mathbf{X}^n_k$. This estimate depends on the actual set of the particles $\mathbf{X}^n_k, n = 1, \dots, N$ that will be sampled by the particle filter using a particle filtering algorithm. A different estimate may be generated at each run of the algorithm even if we fix the true target state $\mathbf{X}_k$ and the random vectors $\mathbf{A}_k = \{A_{l,k}\}^L_{l=1}$ and $\mathbf{v}_k = \{\{v_{u,k}(m)\}^U_{u=1}\}^{M-1}_{m=0}$. This implies that the predicted mean squared error needs to be an average over all possible sets of particles $\mathbf{X}^n_k, n = 1, \dots, N$ that may be sampled by the IPLPF algorithm, as well as an average over possible target states $\mathbf{X}_k$ and set of measurements that were used by the algorithm. The cost function to be minimized with respect to $\mathbf{\Theta}_k$ is:

$$J(\mathbf{\Theta}_k) = E_{\hat{\mathbf{X}}_k,\mathbf{X}_k,\mathbf{A}_k,\mathbf{v}_k|\{\mathbf{X}^n_{k-1}\}^N_{n=1},\mathbf{\Theta}_k}((\mathbf{X}_k - \hat{\mathbf{X}}_k)\mathbf{C}(\mathbf{X}_k - \hat{\mathbf{X}}_k))$$

where the weighting matrix $\mathbf{C}$ [9] makes the units of the cost function consistent.

We denote each possible outcome of the particle filter with index n_p out of N_p possible outcomes as the set of N weight-particle pairs $\{\Gamma^n_{n_p,k}, \mathbf{X}^n_{n_p,k}\}, n = 1, \dots, N$ with corresponding delay-Doppler locations $\{\tau^n_{n_p,\lambda,u,k}, \nu^n_{n_p,\lambda,u,k}\}, \lambda = 1, \dots, \Lambda$. These N pairs for each n_p yield estimates $\hat{\mathbf{X}}_{n_p,k} = \sum^N_{n=1} \Gamma^n_{n_p,k} \mathbf{X}^n_{n_p,k}$. In order to generate predicted true states for evaluating the cost function, we consider the kinematic prior and the particles of the previous time step, similarly to proposing particles. Therefore, we have $N_x = N \times N_p$ possible true states that coincide with the delay-Doppler locations of the possible sampled particles $\mathbf{X}^n_{n_p,k}, n = 1, \dots, N$. We denote predicted true states by $\mathbf{X}_{n_x,k}$.

From the above, we may rewrite the cost function as

$$J(\mathbf{\Theta}_k) = \int\int \sum^{N_x}_{n_x=1} \sum^{N_p}_{n_p=1_N} (\mathbf{X}_{n_x,k} - \sum^N_{n=1} \Gamma^n_{n_p,k}\mathbf{X}^n_{n_p,k})\mathbf{C} \cdot (\mathbf{X}_{n_x,k} - \sum^N_{n=1} \Gamma^n_{n_p,k}\mathbf{X}^n_{n_p,k}) \cdot p(\{\Gamma^n_{n_p,k}, \mathbf{X}^n_{n_p,k}\}^N_{n=1}|\mathbf{X}_{n_x,k}, \mathbf{A}_k, \mathbf{v}_k, \{\mathbf{X}^n_{k-1}\}^N_{n=1}, \mathbf{\Theta}_k) \cdot p(\mathbf{X}_{n_x,k}|\{\mathbf{X}^n_{k-1}\}^N_{n=1}) p(\mathbf{A}_k) p(\mathbf{v}_k) d\mathbf{A}_k d\mathbf{v}_k.$$

When we write the cost function in terms of the expression for the ambiguity function, we conclude [7] that the terms that minimize the AF sidelobes where weak targets exist minimize the cost function. Therefore, we minimize the alternative cost function

$$\bar{J}(\mathbf{\Theta}_k) = |\sum^L_{l=1} \sum^\Lambda_{\lambda=1,\lambda\neq l} \sum^U_{u=1} \sum^{I_\tau}_{i_\tau=0} \sum^{I_\tau}_{i'_\tau=0} \sum^{I_\nu}_{i_\nu=0} \sum^{I_\nu}_{i'_\nu=0} \mathcal{A}_{\mathbf{\Theta}_k}(\tau_{i'_\tau,\lambda,u,k} - \tau_{i_\tau,l,u,k}, \nu_{i_\nu,l,u,k} - \nu_{i'_\nu,\lambda,u,k})|^2.$$

using exhaustive search over the set of values that we choose for $\mathbf{\Theta}_k$. Evaluating the above expression is much less computationally expensive than minimizing $J(\mathbf{\Theta}_k)$.

V. Simulation Results

We use a scenario with one weak target and two strong targets to demonstrate the performance in tracking multiple targets with a) a SCPC Björck CAZAC, b) a non-adapted MCPC Björck CAZAC and c) adaptively configured MCPC Björck CAZACs. Three targets move in a two-dimensional plane. The motion is completed in 199 time steps. Three sensors located at $\chi_1 = -1000$ m, $\psi_1 = 500$ m, $\chi_2 = 2500$ m, $\psi_2 = 500$ m, and $\chi_3 = 500$ m, $\psi_3 = 0$ m collect range and range rate measurements. The trajectory of the target and the location of the sensors are shown in Figure 2. The target

is assumed to move according to a nearly constant velocity model with covariance matrix Q =diag(225 64 225 64).

The weak target $l = 2$ has a cross-sectional area such that it is observed with SNR that varies as $5, 10, 12, 15, 17, 20$ dB. These SNR values correspond to $\sigma^2_{A,2} = [3.16, 10.00, 15.85, 31.63, 50.12, 100.00]$, while we let the strong targets to be characterized by $\sigma^2_{A,1} = \sigma^2_{A,3} = \sigma^2_{A,2} + 1600$. The noise variance is set to $N_0 = 1$ and the energy of the waveform used is $E_s = 1$.

The SCPC Björck CAZAC has length $M = 1741$ and the MCPC waveforms have parameters that vary as $\{M, Q\} = \{7, 245\}, \{11, 154\}, \{13, 130\}$, $\kappa = 0, 1$. For the simulations, we used $N = 300$ particles and the results were averaged over 300 Monte Carlo runs.

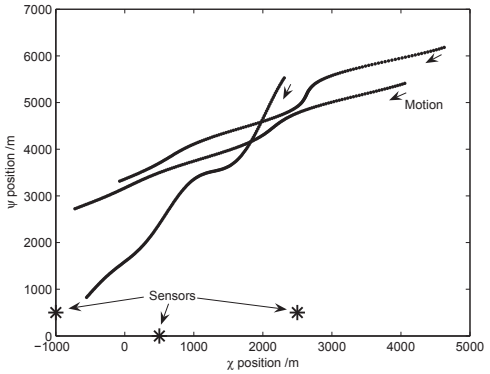

Fig. 2. Target trajectory and sensor location.

The RMSE tracking performance is shown in Figure 3 for different values of SNR and for all waveforms. The percentage of lost tracks is shown for each waveform and SNR value in Figure 4. We observe that the MCPC waveform with adaptive configuration (indicated as AMCPC in all figures) clearly outperforms the SCPC Björck CAZAC and fixed MCPC waveform when considering the number of lost tracks.

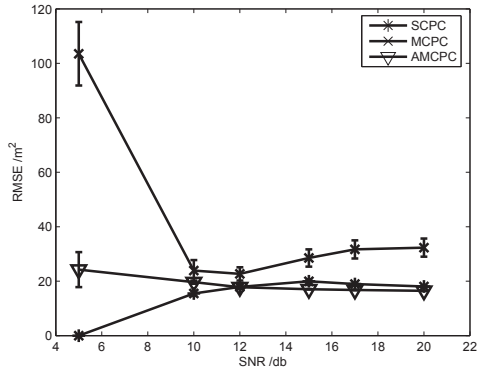

Fig. 3. RMSE versus SNR for the three waveforms with 95% confidence intervals when tracking a weak target and two strong targets.

VI. Conclusions

In this work, we developed the IPLPF algorithm, to track a fixed and known number of targets. Moreover, we developed

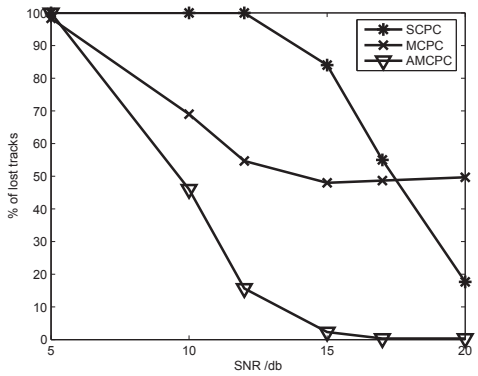

Fig. 4. Percentage of lost tracks versus SNR for the three waveforms when tracking a weak target and two strong targets.

configurable waveforms and an adaptive method that selects waveform parameters such that weak target measurements are unmasked in the presence of strong target measurements. We demonstrated with simulations that when tracking targets with significant difference in strength with fixed waveforms the tracking performance deteriorates. On the other hand the use of adaptively configurable waveforms unmasks weak target measurements and dramatically improves tracking performance.

References

[1] C. Rago, P. Willett, Y. Bar-Shalom, "Detection-Tracking Performance With Combined Waveforms," *IEEE Trans. on Aerospace and Electronic Systems,* vol. 34, no. 2, pp. 612 - 624, April 1998.

[2] D. J. Kershaw and R. J. Evans, "Optimal Waveform Selection for Tracking Systems," *IEEE Trans. Inform. Theory*, vol. 40, no. 5, pp. 1536-1550, Sep. 1994.

[3] M. Orton and W. Fitzgerald, "A Bayesian Approach to Tracking Multiple Targets Using Sensor Arrays and Particle Filters," *IEEE Transactions on Signal Processing*, vol. 50, no. 2, pp. 216-223, Feb. 2002.

[4] M. S. Arulampalam, S. Maskell, N. Gordon, and T. Clapp "A Tutorial on Particle Filters for Online Nonlinear/Non-Gaussian Bayesian Tracking", *IEEE Transactions on Signal Processing*, vol. 50, no. 2, pp. 174-188, Feb. 2002.

[5] N. Levanon and E. Mozeson, *Radar Signals,* Wiley, 2004.

[6] J.J. Benedetto, J. Donatelli, I. Konstantinidis and C. Shaw, "A Doppler Statistic for Zero Autocorrelation Waveforms," *40th Annual Conference on Information Sciences and Systems*, pp. 1403 - 1407, March 2006.

[7] I. Kyriakides, D. Morrell, and A. Papandreou-Suppappola, "Multiple Target Tracking Using Particle Filtering and Adaptive Multicarrier Phase-Coded CAZAC Sequences," IEEE Transactions on Signal Processing, (to be submitted).

[8] G.J. Foster, J.J. Petruzzo III, T.N. Phan, "Track filtering of boosting targets," *Proceedings of the 35th Southeastern Symposium on System Theory*, vol. 35, pp. 450 - 454, March 2003.

[9] S.P. Sira, A. Papandreou-Suppappola and D. Morrell, "Dynamic Configuration of Time-Varying Waveforms for Agile Sensing and Tracking in Clutter," *IEEE Transactions on Signal Processing*, vol. 55, no. 7, pp. 3207-3217, July 2007.

[10] M. I. Skolnik, *Introduction to Radar Systems,* McGraw-Hill, 1980.

[11] E. F. Knott, J. F. Shaeffer, and M. T. Tuley, *Radar Cross Section,* 2nd Edition, SciTech Publishing, 2004.

[12] Ioannis Kyriakides, Darryl Morrell and Antonia Papandreou-Suppappola, "On the Validity of the Measurement Independence Approximation When Using Single and MCPC Waveforms Based on Björck CAZAC Sequences in Multiple Target Radar Tracking With a Particle Filter," Technical Report EEE-5-30-2008-1, ASU, May 2008. http://www.ikyriakides.net.